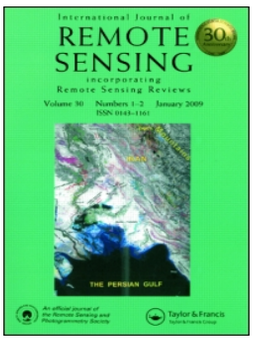

International Journal of Remote Sensing

ISSN: 0143-1161 (Print) 1366-5901 (Online) Journal homepage: http://www.tandfonline.com/loi/tres20

Active learning for object-based image classification using predefined training objects

Lei Ma, Tengyu Fu & Manchun Li

To cite this article: Lei Ma, Tengyu Fu & Manchun Li (2018) Active learning for object-based image classification using predefined training objects, International Journal of Remote Sensing, 39:9, 2746-2765, DOI: 10.1080/01431161.2018.1430398

To link to this article: https://doi.org/10.1080/01431161.2018.1430398

INTERNATIONAL JOURNAL OF REMOTE SENSING, 2018
VOL. 39, NO. 9, 2746–2765
https://doi.org/10.1080/01431161.2018.1430398

Active learning for object-based image classification using predefined training objects

Lei Ma[a,b], Tengyu Fu[a,b] and Manchun Li[a,b]

[a]Jiangsu Provincial Key Laboratory of Geographic Information Science and Technology, Nanjing University, Nanjing, China; [b]School of Geographic and Oceanographic Sciences, Nanjing University, Nanjing, China

ABSTRACT

Object-based image analysis (OBIA) is a new remote-sensing-based image processing technology that has become popular in recent years. In spite of its remarkable advantages, the segmentation results that it generates feature a large number of mixed objects owing to the limitations of OBIA segmentation technology. The mixed objects directly influence the acquisition of training samples and the labelling of objects and thus affect the stability of classification performance. In light of this issue, this article evaluates the influence of classification uncertainty on classification performance and proposes a sampling strategy based on active learning. This sampling strategy is novel in two ways: (1) information entropy is used to evaluate the classification uncertainty of segmented objects; all segmented objects are classified as having zero or non-zero entropies, and the latter are arranged in terms of decreasing entropy. (2) Based on an evaluation of the influence of classification uncertainty on classification performance, an active learning technology is developed. A certain proportion of zero-entropy objects is acquired via random sampling used as seed training samples for active learning, non-zero-entropy objects are used as a candidate set for active learning, and the entropy query-by-bagging (EQB) algorithm is used to conduct active learning to acquire optimal training samples. In this study, three groups of high-resolution images were tested. The test results show that zero-entropy and non-zero-entropy objects are indispensable to the classifier, where the optimal range of the ratio of combination of the two is between 0.2 and 0.6. Moreover, the proposed sampling strategy can effectively improve the stability and accuracy of classification.

ARTICLE HISTORY
Received 13 April 2017
Accepted 8 January 2018

KEYWORDS
Active learning; object-based classification; classification uncertainty; mixed objects; segmentation; sampling

1. Introduction

In recent years, object-based image analysis (OBIA) (Blaschke 2010) has emerged as a new paradigm in the field of sampling and classification of very-high-resolution (VHR) images (Blaschke et al. 2014). OBIA can combine pixels containing the same semantic information as VHR images into a number of meaningful geographical objects. To classify the geographical objects correctly, OBIA creates appropriate mappings by selecting features that are most representative of object classes (Stumpf and Kerle 2011; Ma

CONTACT Lei MA maleinju@nju.edu.cn; Manchun Li, limanchunnju@163.com

et al. 2015). Limited by the segmentation technology of OBIA, however, the geographical objects usually cannot contain pixels belonging to only one land type and thus lead to the over-segmentation and under-segmentation phenomena (Kim et al. 2011). Under-segmentation results in mixed objects in the segmented objects. Such mixed objects degrade class training statistics and, regardless of the class to which the mixed objects are allocated, the allocation is somewhat erroneous (Heumann 2011).

Thus far, a number of studies have considered the issue of segmentation in OBIA (Baatz and Schäpe 2000; Lang et al. 2010; Tiede et al. 2010; Zhang et al. 2013). Nevertheless, researchers have not found an effective solution to the problem of mixed objects. This issue needs urgent resolution in OBIA. On the other hand, given that there are mixed objects in the segmentation results, using mixed objects in training can significantly improve classification accuracy (Costa, Foody, and Boyd 2017). Mixed objects often lie between the relevant classes in feature space and cater to several classes in the feature space; thus, they can provide useful discriminating information for the classifier. However, owing to a lack of prior knowledge, it is difficult to evaluate whether a segmentation object is a mixed object, and the degree of mixing is difficult to calculate. Hence, various uncertainties are encountered when mixed objects are sampled.

Notwithstanding the above issues, OBIA is superior to pixel-based methods in terms of its accuracy of extraction of VHR image information (Myint et al. 2011; Duro, Franklin, and Dubé 2012; Costa et al. 2014). It can also be easily combined with Geographic Information System (GIS) technology to provide all-round land-use-type maps for GIS analysis (Arvor et al. 2013). This makes OBIA a popular method in the field of land coverage and land-use classification (Radoux and Bogaert 2014; Ma et al. 2014). It has garnered widespread attention among researchers (Hay and Castilla 2008; Powers, Hay, and Chen 2012; Arvor et al. 2013; Blaschke et al. 2014; Costa et al. 2014). In past research, many classification algorithms have been proposed to improve the accuracy of object classification. In particular, the algorithms of supervised classification have been extensively researched and incorporated into the OBIA framework (Ma et al. 2017a). Such algorithms include random forest (RF) (Stumpf and Kerle 2011; Puissant, Rougier, and Stumpf 2014; Shruthi et al. 2014; Ma et al. 2017b), *k*-nearest neighbour (Fernández Luque et al., 2013; Tsai, Stow, and Weeks 2011), support vector machines (SVMs) (Heumann 2011; Ma et al. 2017c), decision trees (DTs) (Mallinis et al. 2008), naïve Bayes (Dronova et al. 2012), and neural networks (Rizvi and Mohan 2011).

These supervised classification algorithms have yielded good performance in specific applications. However, every algorithm in supervised classification fluctuates in terms of classification accuracy and quality of training samples (Foody and Arora 1997; Foody 1999; Zhang et al. 2012; Olofsson et al. 2014). To provide classifiers with the correct solution to object classification, it is vital to pick out, of the thousands of samples, the sets of training samples most representative of pixels or objects (Pal and Mather 2003). Although many past studies have attached a lot of importance to sampling strategies for training samples, OBIA in particular is confronted with significant difficulties in the sampling process due to uncertainties concerning segmented objects (Corcoran et al. 2015). Therefore, it is necessary to design a suitable sampling strategy for OBIA with a view to improving the accuracy of subsequent supervised classification as well as its stability.

With regard to machine learning, the sampling problem can be solved through active learning (MacKay 1992; Cohn, Atlas, and Ladner 1994; Cohn, Ghahramani, and Jordan

1996). Active learning is a method to construct an effective training set and is intended to find samples in favour of an improved classification effect via iteration sampling, thus reducing the size of the training set. Active learning is also intended to improve the efficiency of classification algorithms on the premise of limited time and resources. At present, there are three types of commonly used active learning algorithms (Tuia et al. 2009): (1) heuristic methods based on Query by Committee (QBC), (2) heuristic methods based on margin sampling (MS), and (3) heuristic methods based on posterior probability.

Regarding the pixel-based classification of remote-sensing images, a number of methods have been proposed and applied successfully. On the basis of MS-based methods, Mitra, Shankar, and Pal (2004) proposed an SVM MS method similar to object-based image classification and successfully applied it to multispectral imaging through the first Indian Remote Sensing (IRS-1A) satellites. Based on the research findings of Roy and Mccallum (2001), Rajan, Ghosh and Crawford (2008) proposed a probabilistic method for the use of maximum likelihood classifiers that exhibited exceptional performance in Airborne Visible/Infrared imaging spectrometers and Hyperion imaging of the National Aeronautics and Space Administration. In order to enhance the adaptability and performance of active learning algorithms, Tuia et al. (2009) made improvements on MS-based methods (Schohn and Cohn 2000) and the query-by-bagging method and proposed an MS by-closest-support-vector (MS-cSV) and EQB methods; these methods yielded high classification accuracy for VHR imaging in three regions. By using SVM and Linear Discriminant Analysis as classification models, Tuia et al. (2011) evaluated a variety of active learning methods and offered systematic suggestions for the selection of active learning models. The above studies promoted pixel-based active learning methods. However, few studies have considered active learning in OBIA, and researchers have not attended to the active learning strategy that considers mixed objects. In particular, Costa, Foody, and Boyd (2017) confirmed that classification accuracy may benefit from mixed objects by using a cluster sampling strategy but did not explore the effect of using a different sampling strategy.

To sum up, little research has been conducted on sampling strategies for OBIA. This article focuses on improving the performance of object-based supervised classification from the perspective of sampling. Specifically, (1) according to the initial classification results attained by the RF and SVM classifiers, information entropy (Shannon 1938) is calculated to measure the uncertainty of the classification results of segmented objects. (2) According to differences in the uncertainty of classification involving different objects, differentiated sampling strategies are developed for objects with an entropy of zero and those with non-zero entropy through active learning. (3) The final RF classification model is trained and the segmented objects are labelled. The ultimate purpose is to take advantage of the differences between objects with zero entropy and those with non-zero entropies.

2. Study area

In this study, the tested objects included a China unmanned aerial vehicle (UAV) image and the standard data set provided by International Society for Photogrammetry and Remote Sensing (ISPRS) and corresponded to agricultural districts and urban districts,

respectively. The UAV images were acquired from a VHR image acquisition project implemented in Deyang City, Sichuan Province, China (Ma et al. 2013). For this project, a fixed-wing UAV carried Canon EOS 5D Mark II digital cameras; the longitudinal overlap was 80% and the lateral overlap 60%, and the average flight height was 750 m. In August 2011, the digital cameras acquired raw image data for a total area of 400 km^2 distributed in the urban and suburban districts of Deyang City. Using the digital photogrammetry technology, the project personnel finally obtained a digital orthophoto map (DOM) at a resolution ratio of 0.2 m. In this study, we randomly selected a UAV-acquired DOM (500 m × 500 m) in a standard format (as shown in Figure 1(a)), which contained cultivated land (41%), woodlands (46%), rural buildings (6%), rural roads (2%), and bare land (5%).

Released in 2013, the ISPRS standard data set is an open-source data set containing images of urban districts. The entire data set consists of digital aerial image data and airborne laser scanner (ALS) data, as well as the reference layer of each group of images. All data in the data set is available for free at ISPRS' official website (http://www2.isprs.org/commissions/comm3/wg4/tests.html). This study used the digital aerial images for Vaihingen in Germany, acquired and processed by Germany's Association of Photogrammetry and Remote Sensing using Z/I's Digital Mapping Cameras. The resolution ratio of these images was 8 cm (Rottensteiner et al. 2013). Two areas (Areas 28 and 37) were selected for use as experimental areas, and the reference raster layer provided by the

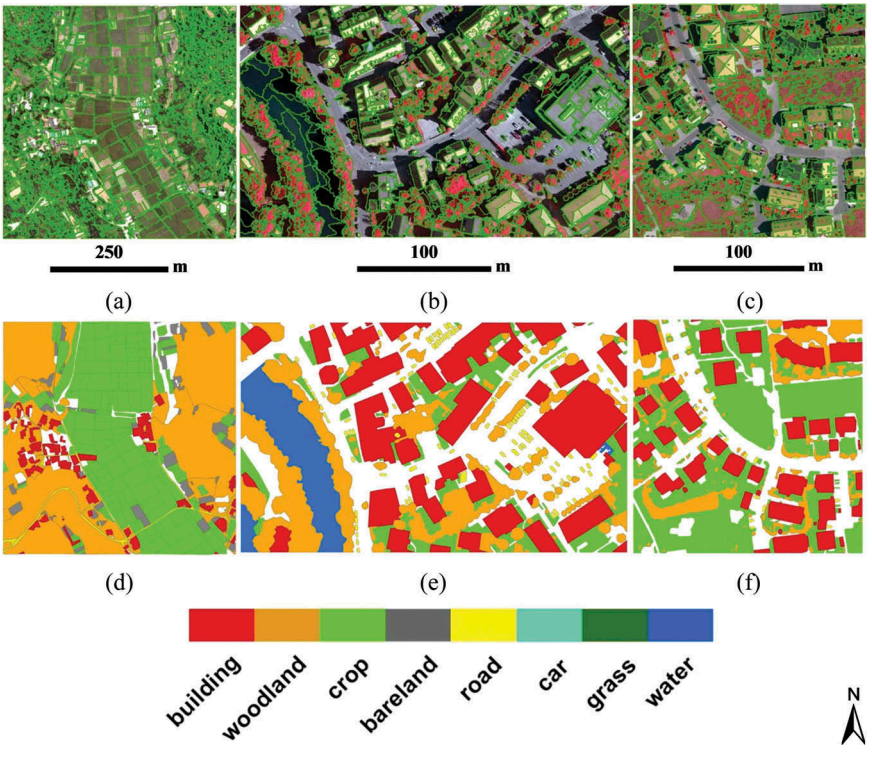

Figure 1. The three study sites used in this article (a, b, and c are the segmented layers of the study sites; the segmentation scale is 130, 110, and 90, respectively; d, e, and f are the corresponding reference layers of the study sites).

ISPRS was vectorized, thus yielding (Figures 1(e and f)). Experimental plot 2 contained buildings (42%), woodlands (29%), bodies of water (12%), cars (3%), and grass (14%). Experimental plot 3 contained buildings (30%), woodlands (18%), cars (1%), and grass (51%). Figures 1(b) and (c)) show the VHR remote-sensing images and segmentation object layers of experimental plots 2 and 3, respectively.

3. Methods

Before describing the proposed sampling strategy, this article first provides a flow chart of the experiment (shown in Figure 2). In the flow chart, Part 1 shows the preprocessing of images or, specifically, the segmentation of the VHR images and generation of the segmented objects (as described in Section 3.1). Part 2 shows the proposed sampling strategy, which is described in detail in Section 3.2. Part 3 shows how to use the final training samples obtained in Part 2 to train the classification model, and how to evaluate the proposed sampling strategy (as described in Sections 3.3 and 3.4).

3.1. *Segmentation*

In object-based image classification, the first step is to segment images and extract the features of the segmented objects. The methods of image segmentation directly influence the effects of image segmentation and the extraction of object features, thus influencing the results of classification (Baatz and Schäpe 2000; Gao et al. 2011; Yang and Kang 2009; Zhang et al. 2015). The multi-resolution segmentation (MRS) algorithm (Baatz and Schäpe 2000) has proved to be a highly successful segmentation algorithm for OBIA (Witharana and Civco 2014; Witharana, Civco, and Meyer 2014). In this study, the MRS algorithm (Baatz and Schäpe 2000) in the eCognition 8.7 software (eCognition Software® Definiens, 2011) was used to segment VHR images. The MRS algorithm is susceptible to human factors. Its main parameters include scale, colour, shape, smoothness, and compactness and are user-defined (Witharana, Civco, and Meyer 2014). Based on experience, the colour parameter was set to 0.9, the shape parameter to 0.1, the smoothness parameter to 0.5, and the compactness parameter was set to 0.5. The scale parameter is the most important parameter in the MRS algorithm (Drăguţ et al. 2014; Hussain et al. 2013; Kim et al. 2011; Myint et al. 2011; Smith 2010). In order to attain optimal classification results for each experimental plot, the segmentation scale of three experimental plots was set to 130, 110, and 90 based on the results of repeated tests.

This article calculated the common shape, texture, and spectral features by using eCongnition 8.7. The shape features included area, density, roundness, compactness, border index, shape index, main direction, elliptic fit, rectangular fit, and asymmetry. The texture features included GLCM entropy, GLCM standard deviation (SD), GLCM contrast, GLCM dissimilarity, GLCM homogeneity, GLCM mean, GLCM angular second moment, and GLCM correlation (they were calculated according to the grey-level co-occurrence matrix [GLCM]) (Haralick, Shanmugam, and Dinstein 1973; Haralick and Shapiro 1985) as well as grey-level difference vector (GLDV) entropy, GLDV contrast, GLDV mean, and GLDV ang.2nd moment (they were calculated according to GLDV) (Weszka, Dyer, and Rosenfeld 1976). The spectral features included mean blue, mean green, mean red, max difference, SD blue, SD green, SD red, and brightness. This article

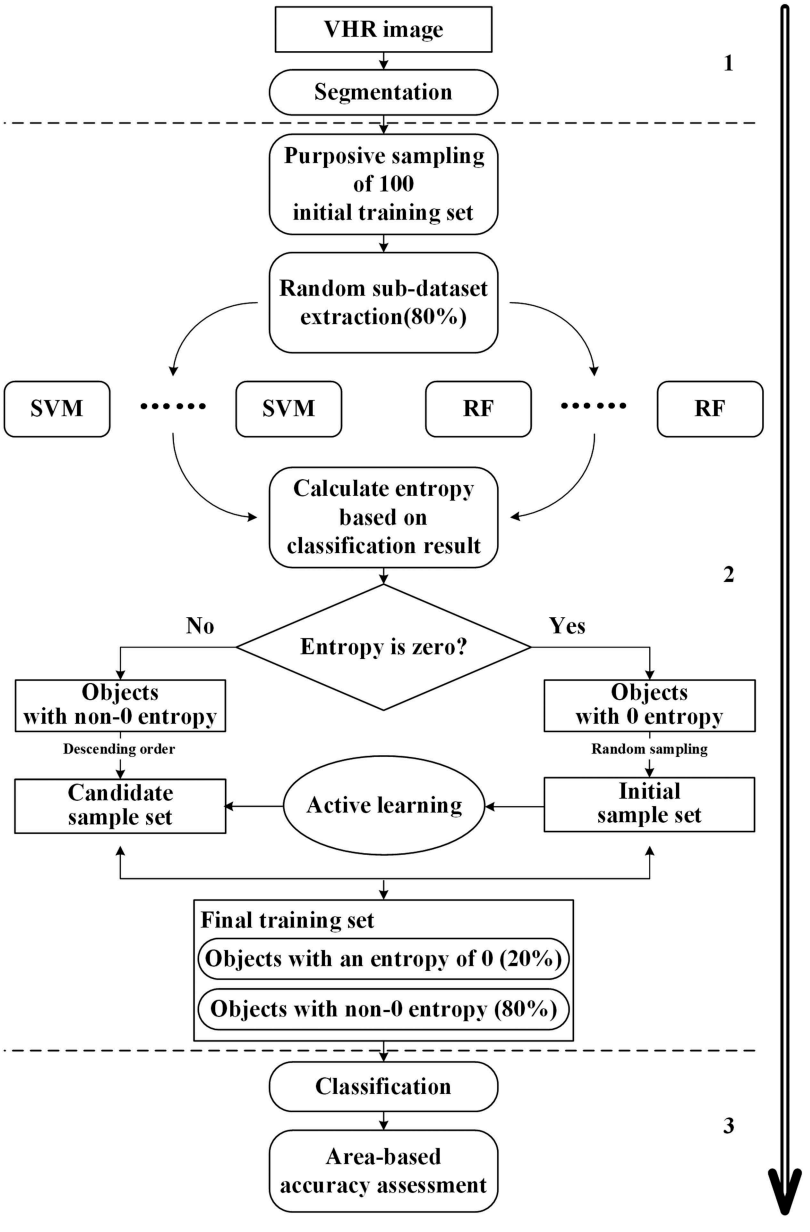

Figure 2. Flow chart of the proposed sampling strategy.

used the class in the major part of a segmentation object to label it (Congalton and Green 2009). If the area of the major part of object exceeded 60% of the total area of the object, the class of the segmentation object was considered consistent with that of the major part. This value of area was employed in this study because it is known to be useful for object-based supervised classification (Verbeeck, Hermy, and Orshoven 2012; Ma et al. 2015).

3.2. *Sampling strategy based on active learning*

3.2.1. *Evaluating classification uncertainty of segmentation object*

Calculating the entropy information of each object consists of two steps: (1) Acquire 100 initial sample objects by stratified random sampling; label them, acquire a subsample set among the labelled samples through stratified random sampling, classify all segmented objects by using the subsample set as a training sample, and record the results of the classification. (2) Acquire subsample sets repeatedly, obtain the results of multiple classifications for the same segmentation object, and collect the classification result-related information of each segmentation object to calculate its information entropy.

The entropy of each object is determined based on its classification results attained by multiple classifiers. Therefore, the pre-labelled 100 samples, which are collected by stratified random sampling method, should ensure that each land type in experimental plot has a sufficient number of samples to train the classification model. Owing to the lack of prior knowledge of the class of each object, a rough proportion of samples for each land type can be confirmed by observing the experimental plot in actual production. Therefore, this proportion does not need to be absolutely accurate but to roughly reflect the land coverage of the experimental plot via visual observation. Subsequently, researchers may acquire 80% of samples from the original training set through random-repetitive sampling with replacement, thus acquiring the training set for each classifier. According to these training sets, this article subsequently used 30 SVM classifiers and 30 RF classifiers to classify all segmented objects and recorded the classification results.

Compared with other classification models, the RF and SVM classifiers provide superior classification effects and higher stability (Li et al. 2016). Therefore, the classification results attained by the SVM and RF classifiers are used to calculate entropy. In this article, the SVM classifier used the LIBSVM library (developed by Chang and Lin 2011) and adopted radial basis function (RBF) (developed by Hsu, Chang, and Lin 2010) as its kernel function. In selecting the penalty parameter C and kernel parameter γ contained in the RBF, the accuracy of each cross validation was tested via grid search, and the parameters with the highest accuracy in cross-validation were selected for use as the penalty parameter and the kernel parameter. The RF classifier is described in detail in Section 3.3.

In Step 2, researchers calculate the information entropy for the classification result of each object. 'Information entropy' (also referred to as 'Shannon entropy') was thus named because Claude Elwood Shannon introduced the concept 'entropy' in thermodynamics to informatics in 1938 (Shannon 1938). Shannon entropy denotes the complexity degree of information. The higher the entropy, the greater the amount of information that can be transferred; the lower the entropy, the less this amount of transferrable information. It has been extensively applied to a diversity of fields and substantially extended. In this article, Shannon entropy is referred to as 'entropy' for short. Entropy is calculated as follows:

$$H = -\sum_{i=1}^{n} p(x_i)\log_2 p(x_i) \tag{1}$$

where $p(x_i)$ is the probability that a segmentation object is labelled as class i, that is the number that the current segmented object is classified as class i divided by the total number of classification repetitions; and n is the number of classes labelled after the

segmentation object is classified 60 times. In this study, the higher the entropy of a segmentation object, the more the number of classes predicted for the segmentation object. If entropy is 0, this indicates that all 60 classifiers predicted the segmentation object as belonging to the same class. Entropy is a relative value and signifies the relative ranking of all segmented objects in each experimental plot. Hence, the lower the entropy, the lower the uncertainty of the classification result of a segmentation object; the higher the entropy, the higher the uncertainty in the classification result of a segmentation object.

3.2.2. *Active learning based on classification uncertainty*

An active learning algorithm (A) may consist of five elements (Settles 2010; Wu et al. 2006) as below:

$$A = (C, \mathrm{L}, S, Q, \mathrm{U}) \tag{2}$$

where C is a classifier or group of classifiers (also referred to as a learning engine), L is a set of labelled training samples, S is an expert who labels the unlabelled samples selected by Q, Q is the query function (also referred to as the sampling engine), which is used to query the samples with the largest amount of information among unlabelled samples, and U is the set of unlabelled samples (also referred to as the set of candidate samples). The active learning algorithm consists of two stages: (1) An initial stage: some samples are randomly selected from among unlabelled samples; the selected samples are labelled by the expert for use as training sample set L and an initial classifier model is built. (2) A cyclic query stage: a certain number of unlabelled samples are selected from among the candidate sample set U in light of query standard Q; the selected unlabelled samples are delivered to S for labelling and added to training sample set L; the classifier is retrained, and the cycle is stopped until training sample set L meets a certain condition.

According to research results obtained by Tuia et al. (2011), the performance of the active learning algorithm depends on the finally selected classification model. Specifically, an MS-based method is suitable for an SVM classifier while a QBC-based method can adapt to most classification models and provide high stability. This article focuses on the test of the proposed sampling strategy rather than the selection of the optimal active learning algorithm. Therefore, this article uses the prevailing EQB algorithm in the QBC-based method for active learning. The EQB algorithm uses the MATLAB Active Learning Toolkit (implemented by Tuia et al. 2011). Based on the results described in Sections 4.1 and 4.2, it set the main parameters of active learning as follows: (1) It randomly drew the zero-entropy objects, which accounted for 20% of the final training samples, for use as the training sample set. (2) Based on entropy, it ranked objects with non-zero entropy in descending order for use as the candidate sample set. The other parameters were set to the default values of the EQB algorithm in the toolkit.

3.3. *Classification*

When object-based remote-sensing image analysis is confronted with various uncertainties, the RF classifier exhibits good adaptability. Also, the SVM classifier is more sensitive to the quality of training samples than the RF classifier (Li et al. 2016). Therefore, the RF classifier was selected as the final classification model to reduce the contingency of the

experiment. The RF consists of multiple DTs that exist independently of one another. The classification results for each DT were used for voting, and the class with the largest number of voting results is the class predicted by the RF (Verikas, Gelzinis, and Bacauskiene 2011). Each DT in the RF was built using bagging technology. When a DT was added, however, the imported *N* features needed to be randomly selected, and the selected *n* features were used as training sample features of the sub-trees. Generally, *n* was far smaller than *N*, and it is recommended that the initial *n* value be equal to $\lfloor \log_2(N) + 1 \rfloor$ or $\sqrt{N}$; subsequently, the *n* value should decrease or increase until out-of-bag (OOB) errors are minimized. The OOB estimate uses the samples not picked out to test random sample subsets (Breiman 2001). Therefore, it was used to measure internal errors to avoid using additional independent testing data sets.

The internal construction of each DT is a process that separates features. It is based on different techniques to measure the importance of each feature in the entire sample set; this process selects the most important feature each time and divides it into a left node and a right node, thus segmenting the training set into smaller subparts recursively. Roughly speaking, constructing an RF classifier requires two parameters: (1) *n*: the number of features when each DT is constructed; (2) *k*: the total number of DTs. In this study, the 'Randomforest' package in R was used. Based on the results obtained by Rodriguez-Galiano et al. (2012), *k* was set to 479 and *n* to one single random segmentation variable, with a view to reduce generalization error and the correlation between trees, and prevent over-fitting in the classification process as much as possible.

3.4. *Accuracy evaluation*

Accuracy evaluation in OBIA is an emerging research area (Blaschke 2010; Radoux et al. 2011; Radoux and Bogaert 2014; Whiteside, Maier, and Boggs 2014). The area-based evaluation method has stood out among the diversity evaluation methods and been extensively applied to accuracy evaluation of buildings (Freire et al. 2014; Shan and Lee 2005). The area-based evaluation method is an operation of the spatial intersection of two data layers (the layer of the classification result and that used as reference), and classification accuracy is the ratio of the area correctly classified to the area of the reference layer. Many previous studies have used this method successfully to assess classification accuracy in OBIA (Ma et al. 2015; Li et al. 2016). We used it as well.

Moreover, Welch's *t*-test (Welch 1947) was used to verify whether there was a significant difference between the two sets of classification accuracy. Welch's *t*-test is an adaptation of Student's *t*-test; that is, it has been derived with the help of Student's *t*-test and is more reliable when two samples have unequal variance and sample size (Ruxton 2006). Student's *t*-test assumes that two populations have a normal distribution with equal variance. Welch's *t*-test is designed for unequal variance but maintains the assumption of normality (Welch 1947). Welch's *t*-test for both sets of data yielded a *p*-value, where there is a significant difference between sets of data when the *p* value is less than 0.05.

4. Results and discussion

4.1. *Classifying segmented objects based on classification uncertainty*

Uncertainty in classification is encountered when objects are difficult to classify. The object that is difficult to classify is often mixed but may be pure. This article used entropy to measure classification uncertainty (Section 3.2.1) to obtain a 'soft' output representing classification uncertainty. In terms of entropy, all segmented objects were classified as objects with zero or non-zero entropies. The numbers of the two types objects under each land type in the three experimental plots are listed in Table 1 to explore the composition of the types of objects.

Table 1 shows that the proportion of objects with zero entropy and non-zero entropy on different land types was different, 1:1.26 for plot 1, 1:0.59 for plot 2, and 1:1.92 for plot 3. They were related to spectral characteristics and an abundance of classes in the classification scene. It was found that the land-cover types of grass and woodland contributed more to the non-zero-entropy objects in plot 3 (Table 1), as it was difficult to recognize both classes due to the similarity in their spectral characteristics. Moreover, the buildings in plot 3 were difficult to classify accurately because the objects were relatively small. Subsequently, the proportion with zero and non-zero entropies was very low (1:1.92) in plot 3 compared to those in the other two plots, whereas these three classes (grass, woodland, and building) covered 99% of plot 3 (Figure 1). Furthermore, the proportion was high (1:0.59) owing to a large number of the zero-entropy objects with woodlands and buildings, as they covered 71% of plot 2 (Figure 1), were easily distinguishable. For plot 1, zero and non-zero-entropy objects were more balanced because the woodlands were detected easily, whereas the other classes were difficult to recognize accurately due to their similar spectra. For example, the crop possibly contained a diversity of annual crops or permanent orchards.

In addition to the above, the distribution of mixed objects in experimental plots also resulted in classification uncertainty, to contribute non-zero-entropy objects. The woodlands are obviously concentrated and contiguous in experimental plots 1 and 2, where

Table 1. Number of objects with zero and non-zero entropy under each land type in the experimental plots.

Study site	Class type	Sample count	Sample count (with zero entropy)	Sample count (with non-zero entropy)
1	Bare land	69	4	65
	Woodland	430	278	152
	Building	109	27	82
	Crop	220	67	153
	Road	27	2	25
		855	378	477
2	Grass	96	23	73
	Woodland	277	194	83
	Building	458	341	117
	Car	49	19	30
	Water	38	1	37
		918	578	340
3	Grass	412	151	261
	Woodland	204	44	160
	Building	368	144	224
	Car	14	3	11
		998	342	656

the polygon of the manual interpretation is relatively large for the area of the woodlands, whereas the segmented woodland objects are usually small (Figure 1 (a,b)). A large number of segmented objects from the woodlands are hence contained in each district corresponding to the woodlands in the reference layer, and thus, the number of pure objects is larger than that of the mixed objects. Similarly, the segmented building objects are usually small. Experimental plot 2 has a large number of large buildings (high-rise residential buildings), and experimental plot 3 contains many small buildings with areas far smaller than that in experimental plot 2. Therefore, in experiment 2, for the buildings, the number of pure objects was larger than that of mixed objects, whereas single buildings were divided into several segmented objects.

The classification of zero-entropy and non-zero-entropy objects varied from one experimental plot to the other, and these changes were related to multiple factors: spectral characteristics, the abundance of classes in each experimental plot, and the degree of mixing. Hence, zero-entropy objects had low classification uncertainty or degree of mixing (including parts of pure objects), and non-zero-entropy objects consisted a large number of mixed objects with highly classification uncertainty.

4.2. *Influence of type of object on classification*

To utilize the significant differences between zero-entropy and non-zero-entropy objects, we ranked the latter objects based on entropy and assigned priority to those with high entropy. Moreover, although the mixed objects were difficult to classify, classification accuracy can significantly improve when using them in training (Costa, Foody, and Boyd 2017). So, our intention of the proposed method also includes the priority sampling of the mixed objects. While non-zero-entropy objects included mixed objects as well as pure objects that were difficult to distinguish, the entropy of such pure objects was close to zero. As pure objects, unlike mixed objects, contain pixels of only one class, it is problematic that they are allocated to multiple classes. Therefore, the entropy of pure objects is close to 0 as they were assigned few classes. In other words, the higher the entropy of an object, the more likely it is to be mixed. Therefore, the proposed strategy adopts the preferential sampling of high-entropy objects.

An optimal classification effect is attained if zero-entropy and non-zero-entropy objects are combined at an appropriate ratio. Therefore, a ratio test was conducted to provide a basis for the active learning strategy, and the results of ratio test are shown in Figure 3. The test rules were as follows: (1) Combine two types of objects at different ratios (zero-entropy objects to final training samples). When the ratio was zero, the final training samples all consisted of objects with non-zero entropy; when the ratio was 1, the final training samples were all objects with zero entropy. (2) In the final training samples, zero-entropy objects were selected by random sampling while non-zero-entropy objects were ranked based on decreasing entropy. Based on these test rules, classification was conducted 20 times for each training sample and, thus, the mean (the *y*-value of each node in Figure 3) and SD (the error bar at each node in Figure 3) of 20 accuracy values were calculated to delineate the pattern of ratios affecting classification accuracy.

In Figure 3, the zero-entropy or non-zero-entropy objects in each experimental plot might sometimes be insufficient in number; therefore, the *x*-coordinate under some ratios was smaller. Moreover, to avoid significant fluctuations in classification accuracy

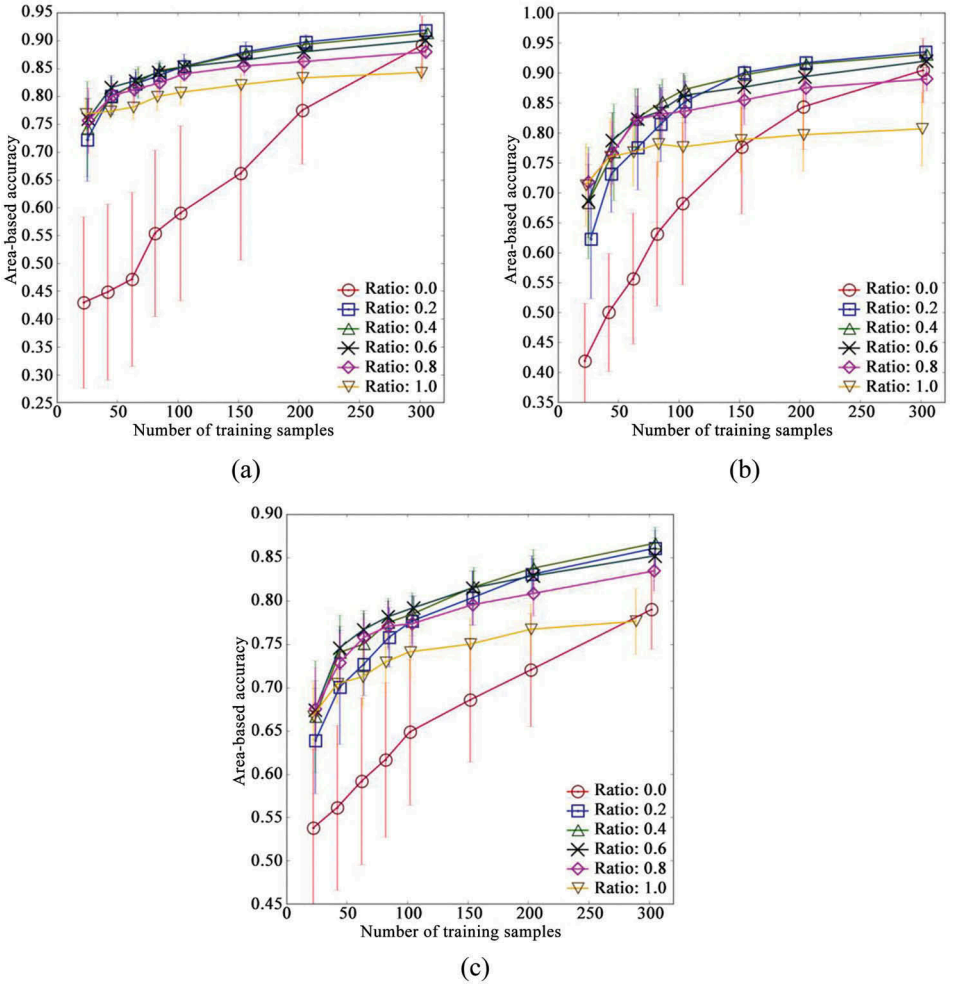

Figure 3. Results of ratio test on different experimental plots. (a) Rural districts of Deyang City in China. (b) District 28 of Vaihingen in Germany. (c) District 37 of Vaihingen in Germany (the *x*-coordinate of the broken line graph denotes the number of training samples, and the *y*-coordinate denotes the classification accuracy attained by the area-based evaluation method. The numbers of training samples at different nodes were 20, 40, 60, 80, 100, 150, 200, and 300).

owing to the small number of classes, a sample at least was added to each missing class when classes containing training samples were incomplete. It can be seen from the ratio test that (1) The range of ratios for optimal classification was between 0.2 and 0.6 (the blue, green, and black lines in Figure 3). (2) When the ratio was zero (red line) and 1 (yellow line), both classification accuracy and stability were far below those under all other ratios. (3) When the number of training samples was below 100, the optimal ratio was 0.6. (4) When the number of training samples was above 200, the ratio of 0.2 usually brought about optimal classification effects.

The higher the classification uncertainty of an object (the higher the entropy), the closer it is to the juncture of different classes in the feature space and hence can provide a more accurate division plan for the classifier. While a zero-entropy object is far from the

juncture of different classes, it can often act as an indicator; for example, it can indicate the inner and outer sides of the hyper-plane of a given class. Therefore, ratios of zero (red line) and 1 (yellow line) are inappropriate (see Figure 3). Further, when the number of training samples was small, the results that classification accuracy with yellow line is higher than that with red line indicated that zero-entropy objects were more advantageous than non-zero-entropy objects. We assumed that the zero-entropy objects helped the classifier find an inaccurate but practical classification solution with small training sample size. As the number of training samples increased, the number of zero-entropy objects increased to a certain size, then the classifier more need training samples of the mixed objects which can provide accurate hyper-plane. Therefore, both zero-entropy and non-zero-entropy objects appear indispensable to the classifier, where the optimal combination range of ratios for the two types of objects is between 0.2 and 0.6.

Based on the above, active learning can be used to overcome the disadvantages of different ratios. Active learning is intended to help the expert select better training samples. If it is used, it is expected that as many candidate samples as possible can be learned by as few initial samples as possible. If the ratio is extremely high, active learning has no significance, and stability decreases. Therefore, this article selected a ratio of 0.2 for active learning. Specifically, zero-entropy objects, which accounted for 20% of the final training samples, were used as the initial training sample set for active learning; non-zero-entropy objects, which were ranked by entropy in descending order, were used as a candidate sample set for active learning.

4.3. *Improving classification by active learning*

In Figure 4, the RS curve (red line) shows that classification accuracy was obtained by using random sampling. The EQB curve (blue line) shows the results based on the samples in Table 1 using the strategy proposed in this article (Section 3.2.2) 10 times, to obtain the mean value and the SD. The curve for a ratio of 0.2 (green line) shows the results of the ratio test described in Section 4.2. The error bar at each node represents the SD of multiple classification accuracy values. As shown in Figure 4, the effect of classification at a ratio of 0.2 (green line) was not superior to that obtained by using random sampling, especially in experimental plot 3. Therefore, active learning was needed. Table 2 lists the results of Welch's *t*-test, which was performed at values between the EQB curve and the RS curve.

Combining Table 2 and Figure 4, we see that compared with random sampling, the proposed strategy exhibited satisfactory classification effects on the three experimental plots when the sample size was above 100. When the number of training samples was greater than 150, the fluctuation in classification accuracy was close to 1%. This represented a significant improvement over random sampling. In a small sample size range (below 100), however, the sampling strategy proposed here had no remarkable advantage over random sampling. There are two reasons for this: (1) The EQB algorithm is not suitable for a range over a small sample size (Tuia et al. 2011). (2) The proposed strategy involves learning non-zero-entropy objects with high entropies in preference over others. In several initial recursions, the non-zero-entropy objects were all learned owing to the large differences between the two object types. Therefore, the full

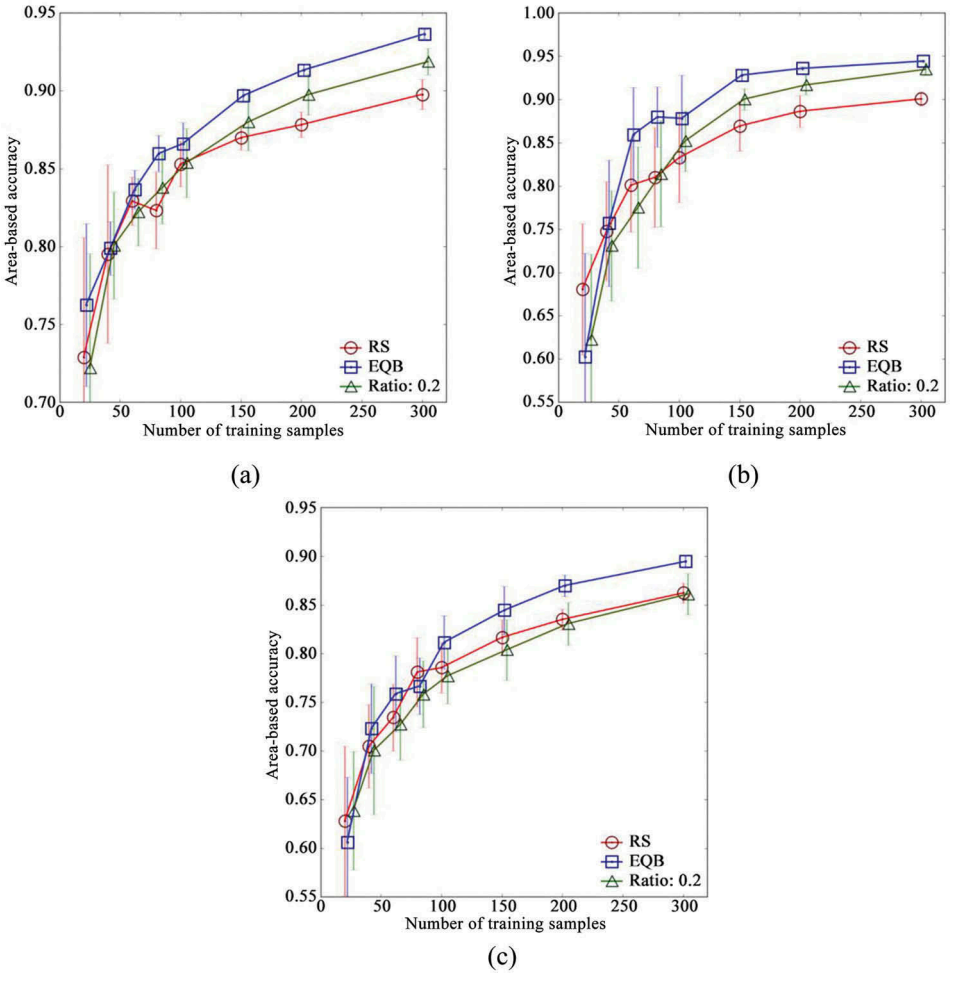

Figure 4. Classification accuracy curves for study sites. (a) Rural districts of Deyang City in China. (b) District 28 of Vaihingen in Germany. (c) District 37 of Vaihingen in Germany (the *x*-coordinate of the broken line graph denotes the number of training sample sets used to finally train the RF classifier, and the *y*-coordinate denotes the classification accuracy attained via the area-based evaluation; the numbers of training samples at different nodes were 20, 40, 60, 80, 100, 150, 200, and 300. RS refers to random sampling and EQB to entropy query-by-committee).

advantage of active learning cannot be exercised to select samples with the largest amounts of information.

Figure 5 shows the classification effect of the three experimental plots when the number of training samples was 200. In experimental plot 1, the proposed sampling strategy (shown in g) attained a good classification effect for two land types, bare lands (grey) and buildings (red). In experimental plot 2, the proposed sampling strategy (shown in h) significantly improved classification accuracy for grass (dark green) and waterbodies (blue). In experimental plot 3, random sampling (shown in f) yielded a chaos of classification of some buildings; by contrast, the proposed strategy satisfactorily improved the classification accuracy for buildings (red). This is because the proposed

Table 2. The results of Welch's *t*-test for the proposed strategy and random sampling.

Study site 1								
Sample count	20	40	60	80	100	150	200	300
EQB/RS (*p* value)	>0.05	>0.05	>0.05	<0.05	<0.05	<0.05	<0.05	<0.05
Study site 2								
Sample count	20	40	60	80	100	150	200	300
EQB/RS (*p* value)	>0.05	>0.05	<0.05	<0.05	<0.05	<0.05	<0.05	<0.05
Study site 3								
Sample count	20	40	60	80	100	150	200	300
EQB/RS (*p* value)	>0.05	>0.05	>0.05	>0.05	<0.05	<0.05	<0.05	<0.05

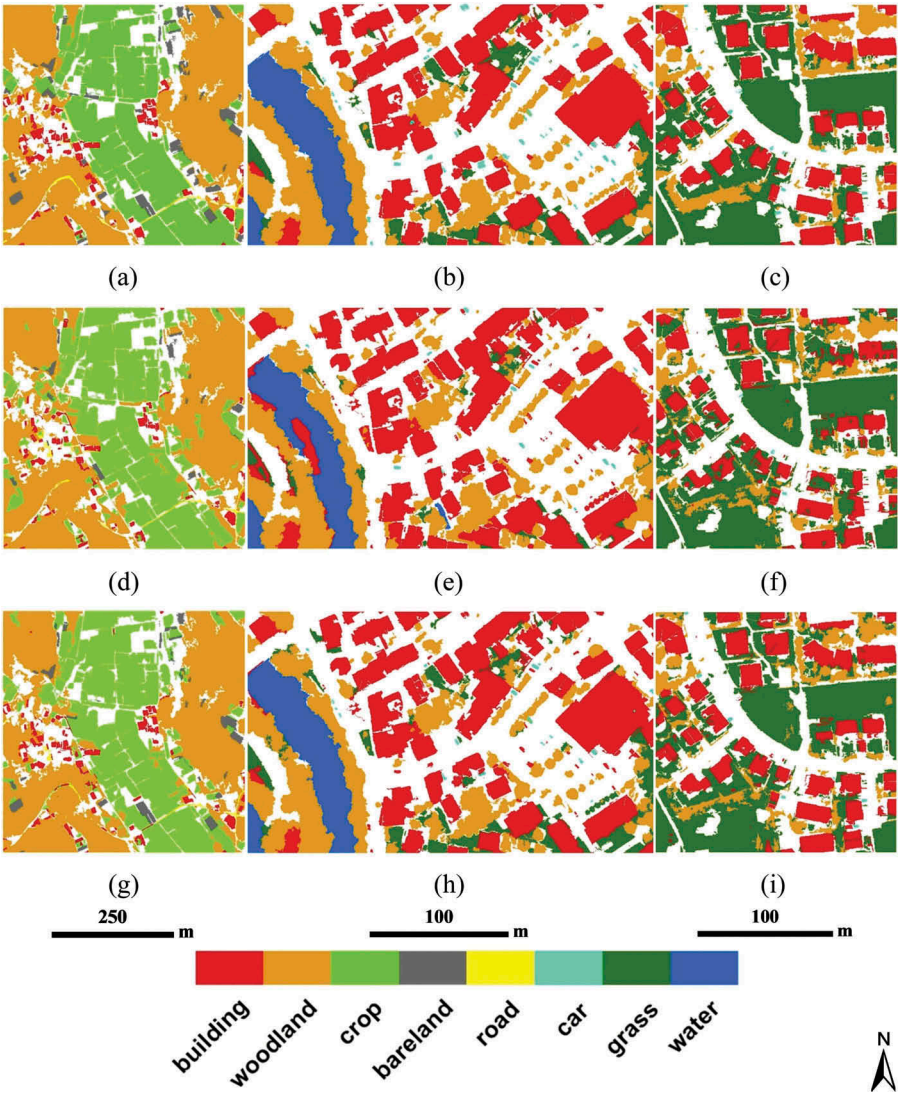

Figure 5. The classification effect on the three experimental plots when the number of training samples was 200 (a, b, and c show the vector layers on correct segmented objects in three experimental plots; d, e, and f show the vector layers on the classification of all segmented objects after random sampling; g, h, and i show the vector layers on the classification of segmented objects by using the sampling strategy proposed here).

strategy uses the difference between zero-entropy and non-zero-entropy object and takes advantage of the fact that mixed objects can improve classification (Costa, Foody, and Boyd 2017). Hence, preferentially sampling mixed objects with high classification uncertainty by active learning is useful in this regard.

5. Conclusions

This article proposed a novel sampling strategy for OBIA that uses active learning to sample training objects to help improve sampling efficiency for the classification of OBIA and attain a representative training sample set. The influence of classification uncertainty (calculated by entropy) on sampling was first calculated, and the following conclusion were drawn: (1) zero-entropy and non-zero-entropy objects are indispensable to the classifier, and the optimal range of the combination of ratios for the two types of objects is between 0.2 and 0.6. (2) When the number of training samples is small, zero-entropy objects are more effective in improving accuracy. (3) When the number of training samples is large, non-zero-entropy objects are more effective in improving accuracy. This article also proposed the following active learning strategy: zero-entropy objects, which accounted for 20% of the final training samples, were used to learn non-zero-entropy objects, which accounted for 80%, with a view to attaining a stable final training sample set. The experimental results showed that the proposed sampling strategy improved classification and the stability of classification accuracy compared with random sampling. Therefore, in terms of classification performance, the proposed strategy is an excellent sampling solution. However, it still remains to be explored from many aspects. In this study, supervised classification was used to calculate the entropy of each segmentation object. In future work, an unsupervised classification approach should be explored to calculate the entropy, thus saving the initial 100 training samples. Moreover, computational complexity can be reduced with the use of an iterative process through parallel technologies.

Acknowledgements

This work was supported by the National Natural Science Foundation of China: [Grant Number 41701374], the Natural Science Foundation of Jiangsu Province of China: [Grant Number BK20170640], the National Key R&D Program of China: [Grant Number 2017YFB0504205], and the China Postdoctoral Science Foundation [Grant Number 2017T10034, 2016M600392]. We are also grateful to anonymous reviewers and members of the editorial team for advice.

Disclosure statement

No potential conflict of interest was reported by the authors.

Funding

This work was supported by National Natural Science Foundation of China: [Grant Number 41701374]; Natural Science Foundation of Jiangsu Province of China: [Grant Number BK20170640]; National Key R&D Program of China: [Grant Number 2017YFB0504205]; China Postdoctoral Science Foundation: [Grant Number 2016M600392, 2017T10034].

References

Arvor, D., L. Durieux, S. Andrés, and M. A. Laporte. 2013. "Advances in Geographic Object-Based Image Analysis with Ontologies: A Review of Main Contributions and Limitations from A Remote Sensing Perspective." *ISPRS Journal of Photogrammetry and Remote Sensing* 82 (8): 125–137. doi:10.1016/j.isprsjprs.2013.05.003.

Baatz, M., and A. Schäpe. 2000. "Multiresolution Segmentation–An Optimization Approach for High-Quality Multi-Scale Image Segmentation." *Journal of Photogrammetry and Remote Sensing* 58: 12–23.

Blaschke, T. 2010. "Object-Based Image Analysis for Remote Sensing." *ISPRS Journal of Photogrammetry and Remote Sensing* 65 (1): 2–16. doi:10.1016/j.isprsjprs.2009.06.004.

Blaschke, T., G. J. Hay, M. Kelly, S. Lang, P. Hofmann, E. Addink, R. Q. Feitosa, et al. 2014. "Geographic Object-Based Image Analysis–Towards a New Paradigm." *ISPRS Journal of Photogrammetry and Remote Sensing* 87 (100): 180–191. DOI:10.1016/j.isprsjprs.2013.09.014.

Breiman, L. 2001. "Random Forests." *Machine Learning* 45 (1): 5–32. doi:10.1023/A:1010933404324.

Chang, C. C., and C. J. Lin. 2011. "LIBSVM: A Library for Support Vector Machines." *ACM Transactions on Intelligent Systems and Technology* 2 (27): 1–27. doi:10.1145/1961189.1961199.

Cohn, D., L. Atlas, and R. Ladner. 1994. "Improving Generalization with Active Learning." *Machine Learning* 15 (2): 201–221. doi:10.1007/BF00993277.

Cohn, D. A., Z. Ghahramani, and M. I. Jordan. 1996. "Active Learning with Statistical Models." *Journal of Artificial Intelligence Research* 4 (1): 129–145.

Congalton, R. G., and K. Green. 2009. *Assessing the Accuracy of Remotely Sensed Data: Principles and Practices*. 2nd ed. Boca Raton, FL: CRC Press.

Corcoran, J., J. Knight, K. Pelletier, L. Rampi, and Y. Wang. 2015. "The Effects of Point or Polygon Based Training Data on Random Forest Classification Accuracy of Wetlands." *Remote Sensing* 7 (4): 4002–4025. doi:10.3390/rs70404002.

Costa, H., G. M. Foody, and D. S. Boyd. 2017. "Using Mixed Objects in the Training of Object-Based Image Classifications." *Remote Sensing of Environment* 190: 188–197. doi:10.1016/j.rse.2016.12.017.

Costa, H., H. Carrao, F. Bacao, and M. Caetano. 2014. "Combining Per-Pixel and Object-Based Classifications for Mapping Land Cover over Large Areas." *International Journal of Remote Sensing* 35 (2): 738–753. doi:10.1080/01431161.2013.873151.

Drăguţ, L., O. Csillik, C. Eisank, and D. Tiede. 2014. "Automated Parameterisation for Multi-Scale Image Segmentation on Multiple Layers." *ISPRS Journal of Photogrammetry and Remote Sensing* 88 (100): 119–127. doi:10.1016/j.isprsjprs.2013.11.018.

Dronova, I., P. Gong, N. E. Clinton, L. Wang, W. Fu, S. Qi, and Y. Liu. 2012. "Landscape Analysis of Wetland Plant Functional Types: The Effects of Image Segmentation Scale, Vegetation Classes and Classification Methods." *Remote Sensing of Environment* 127 (140): 357–369. doi:10.1016/j.rse.2012.09.018.

Duro, D. C., S. E. Franklin, and M. G. Dubé. 2012. "A Comparison of Pixel-Based and Object-Based Image Analysis with Selected Machine Learning Algorithms for the Classification of Agricultural Landscapes Using SPOT-5 HRG Imagery." *Remote Sensing of Environment* 118 (6): 259–272. doi:10.1016/j.rse.2011.11.020.

Fernández Luque, I., F. J. Aguilar, M. F. Álvarez, and M. Á. Aguilar. 2013. "Non-Parametric Object-Based Approaches to Carry Out ISA Classification from Archival Aerial Orthoimages." *IEEE Journal of Selected Topics in Applied Earth Observations & Remote Sensing* 6 (4): 2058–2071. doi:10.1109/JSTARS.2013.2240265.

Foody, G. M. 1999. "The Significance of Border Training Patterns in Classification by a Feedforward Neural Network Using Back Propagation Learning." *International Journal of Remote Sensing* 20 (18): 3549–3562. doi:10.1080/014311699211192.

Foody, G. M., and M. K. Arora. 1997. "An Evaluation of Some Factors Affecting the Accuracy of Classification by an Artificial Neural Network." *International Journal of Remote Sensing* 18 (4): 799–810. doi:10.1080/014311697218764.

Freire, S., T. Santos, A. Navarro, F. Soares, J. D. Silva, N. Afonso, A. Fonseca, and J. Tenedório. 2014. "Introducing Mapping Standards in the Quality Assessment of Buildings Extracted from Very

High Resolution Satellite Imagery." *ISPRS Journal of Photogrammetry and Remote Sensing* 90 (4): 1–9. doi:10.1016/j.isprsjprs.2013.12.009.

Gao, Y., J. F. Mas, N. Kerle, and J. A. N. Pacheco. 2011. "Optimal Region Growing Segmentation and Its Effect on Classification Accuracy." *International Journal of Remote Sensing* 32 (13): 3747–3763. doi:10.1080/01431161003777189.

Haralick, R., and L. Shapiro. 1985. "Image Segmentation Techniques." *Computer Vision, Graphics and Image Processing* 29 (1): 100–132. doi:10.1016/S0734-189X(85)90153-7.

Haralick, R. M., K. Shanmugam, and I. H. Dinstein. 1973. "Textural Features for Image Classification." *IEEE Transactions on Systems, Man and Cybernetics*, no. 6: 610–621. doi:10.1109/TSMC.1973.4309314.

Hay, G. J., and G. Castilla. 2008. "Geographic Object-Based Image Analysis (GEOBIA): A New Name for a New Discipline." In *Object-Based Image Analysis*, edited by T. Blaschke, S. Lang, and G. Hay, 75–89. Berlin, Heidelberg: Springer.

Heumann, B. W. 2011. "An Object-Based Classification of Mangroves Using a Hybrid Decision Tree Support Vector Machine Approach." *Remote Sensing* 3 (11): 2440–2460. doi:10.3390/rs3112440.

Hsu, C. W., C. C. Chang, and C. J. Lin. 2010. "A Practical Guide to Support Vector Classification." *Bioinformatics* 1: 1–16.

Hussain, M., D. M. Chen, A. Cheng, H. Wei, and D. Stanley. 2013. "Change Detection from Remotely Sensed Images: From Pixel-Based to Object-Based Approaches." *ISPRS Journal of Photogrammetry and Remote Sensing* 80 (2): 91–106. doi:10.1016/j.isprsjprs.2013.03.006.

Kim, M., T. A. Warner, M. Madden, and D. S. Atkinson. 2011. "Multi-Scale GEOBIA with Very High Spatial Resolution Digital Aerial Imagery: Scale, Texture, and Image Objects." *International Journal of Remote Sensing* 32 (10): 2825–2850. doi:10.1080/01431161003745608.

Lang, S., F. Albrecht, S. Kienberger, and D. Tiede. 2010. "Object Validity for Operational Tasks in a Policy Context." *Journal of Spatial Science* 55 (1): 9–22. doi:10.1080/14498596.2010.487639.

Li, M., L. Ma, T. Blaschke, L. Cheng, and D. Tiede. 2016. "A Systematic Comparison of Different Object-Based Classification Techniques Using High Spatial Resolution Imagery in Agricultural Environments." *International Journal of Applied Earth Observation and Geoinformation* 49: 87–98. doi:10.1016/j.jag.2016.01.011.

Ma, L., L. Cheng, M. Li, Y. Liu, and X. Ma. 2015. "Training Set Size, Scale, and Features in Geographic Object-Based Image Analysis of Very High Resolution Unmanned Aerial Vehicle Imagery." *ISPRS Journal of Photogrammetry & Remote Sensing* 102: 14–27. doi:10.1016/j.isprsjprs.2014.12.026.

Ma, L., L. Cheng, W. Han, L. Zhong, and M. Li. 2014. "Cultivated Land Information Extraction from High-Resolution Unmanned Aerial Vehicle Imagery Data." *Journal of Applied Remote Sensing* 8 (83673): 1–25. doi:10.1117/1.JRS.8.083673.

Ma, L., M. Li, L. Tong, Y. Wang, and L. Cheng. 2013. "Using Unmanned Aerial Vehicle for Remote Sensing Application." In *2013 21st International Conference on Geoinformatics*, pp. 1–5. Kaifeng, China.

Ma, L., M. Li, X. Ma, L. Cheng, P. Du, and Y. Liu. 2017a. "A Review of Supervised Object-Based Land-Cover Image Classification." *ISPRS Journal of Photogrammetry and Remote Sensing* 130: 277–293. doi:10.1016/j.isprsjprs.2017.06.001.

Ma, L., M. Li, Y. Gao, T. Chen, X. Ma, and L. Qu. 2017c. "A Novel Wrapper Approach for Feature Selection in Object-Based Image Classification Using Polygon-Based Cross-Validation." *IEEE Geoscience and Remote Sensing Letters* 14 (3): 409–413. doi:10.1109/LGRS.2016.2645710.

Ma, L., T. Fu, T. Blaschke, M. Li, T. Dirk, Z. Zhou, X. Ma, and D. Chen. 2017b. "Evaluation of Feature Selection Methods for Object-Based Land Cover Mapping of Unmanned Aerial Vehicle Imagery Using Random Forest and Support Vector Machine Classifiers." *ISPRS International Journal of Geo-Information* 6 (2): 51. doi:10.3390/ijgi6020051.

MacKay, D. J. C. 1992. "Information-Based Objective Functions for Active Data Selection." *Neural Computation* 4 (4): 590–604. doi:10.1162/neco.1992.4.4.590.

Mallinis, G., N. Koutsias, M. Tsakiri-Strati, and M. Karteris. 2008. "Object-Based Classification Using Quickbird Imagery for Delineating Forest Vegetation Polygons in a Mediterranean Test Site." *ISPRS Journal of Photogrammetry and Remote Sensing* 63 (3): 237–250. doi:10.1016/j.isprsjprs.2007.08.007.

Mitra, P., B. U. Shankar, and S. K. Pal. 2004. "Segmentation of Multispectral Remote Sensing Images Using Active Support Vector Machines." *Pattern Recognition Letters* 25 (9): 1067–1074. doi:10.1016/j.patrec.2004.03.004.

Myint, S. W., P. Gober, A. Brazel, S. Grossman-Clarke, and Q. Weng. 2011. "Per-Pixel Vs. Object-Based Classification of Urban Land Cover Extraction Using High Spatial Resolution Imagery." *Remote Sensing of Environment* 115 (5): 1145–1161. doi:10.1016/j.rse.2010.12.017.

Olofsson, P., G. M. Foody, M. Herold, S. V. Stehman, C. E. Woodcock, and M. A. Wulder. 2014. "Good Practices for Estimating Area and Assessing Accuracy of Land Change." *Remote Sensing of Environment* 148 (5): 42–57. doi:10.1016/j.rse.2014.02.015.

Pal, M., and P. M. Mather. 2003. "An Assessment of the Effectiveness of Decision Tree Methods for Land Cover Classification." *Remote Sensing of Environment* 86 (4): 554–565. doi:10.1016/S0034-4257(03)00132-9.

Powers, R. P., G. J. Hay, and G. Chen. 2012. "How Wetland Type and Area Differ through Scale: A GEOBIA Case Study in Alberta's Boreal Plains." *Remote Sensing of Environment* 117: 135–145. doi:10.1016/j.rse.2011.07.009.

Puissant, A., S. Rougier, and A. Stumpf. 2014. "Object-Oriented Mapping of Urban Trees Using Random Forest Classifiers." *International Journal of Applied Earth Observations & Geoinformation* 26 (1): 235–245. doi:10.1016/j.jag.2013.07.002.

Radoux, J., and P. Bogaert. 2014. "Accounting for the Area of Polygon Sampling Units for the Prediction of Primary Accuracy Assessment Indices." *Remote Sensing of Environment* 142: 9–19. doi:10.1016/j.rse.2013.10.030.

Radoux, J., P. Bogaert, D. Fasbender, and P. Defourny. 2011. "Thematic Accuracy Assessment of Geographic Object-Based Image Classification." *International Journal of Geographical Information Science* 25 (6): 895–911. doi:10.1080/13658816.2010.498378.

Rajan, S., J. Ghosh, and M. M. Crawford. 2008. "An Active Learning Approach to Hyperspectral Data Classification." *IEEE Transactions on Geoscience and Remote Sensing* 46 (4): 1231–1242. doi:10.1109/TGRS.2007.910220.

Rizvi, I. A., and B. K. Mohan. 2011. "Object-Based Image Analysis of High-Resolution Satellite Images Using Modified Cloud Basis Function Neural Network and Probabilistic Relaxation Labelling Process." *IEEE Transactions on Geoscience & Remote Sensing* 49 (12): 4815–4820. doi:10.1109/TGRS.2011.2171695.

Rodriguez-Galiano, V. F., B. Ghimire, J. Rogan, M. Chica-Olmo, and J. P. Rigol-Sanchez. 2012. "An Assessment of the Effectiveness of a Random Forest Classifier for Land-cover Classification." *ISPRS Journal of Photogrammetry and Remote Sensing* 67: 93-104. doi:10.1016/j.isprsjprs.2011.11.002.

Rottensteiner, F., G. Sohn, M. Gerke, and J. D. Wegner. 2013. "ISPRS Test Project on Urban Classification and 3D Building Reconstruction." *Commission III-Photogrammetric Computer Vision and Image Analysis*, *Working Group III/4-3D Scene Analysis*: 1–17.

Roy, N., and A. Mccallum. 2001. "Toward Optimal Active Learning through Sampling Estimation of Error Reduction." Proceedings of 18th International Conference on Machine Learning, Williamstown, MA, June 28–July 1, 441–448.

Ruxton, G. D. 2006. "The Unequal Variance *T*-Test Is an Underused Alternative to Student's *T*-Test and the Mann–Whitney U Test." *Behavioral Ecology* 17 (4): 688–690. doi:10.1093/beheco/ark016.

Schohn, G., and D. Cohn. 2000. "Less is More: Active Learning with Support Vector Machines." In *Proceedings of the Seventeenth International Conference on Machine Learning*, edited by Pat Langley, Stanford University, CA, June 29-July 2, 839–846. Burlington, MA: Morgan Kaufmann Publishers.

Settles, B. 2010. *Active Learning Literature Survey*. Computer Sciences Technical Report 1648. Madison, WI: University of Wisconsin Madison.

Shan, J., and S. D. Lee. 2005. "Quality of Building Extraction from IKONOS Imagery." *Journal of Surveying Engineering* 131 (1): 27–32. doi:10.1061/(ASCE)0733-9453(2005)131:1(27).

Shannon, C. E. 1938. "A Symbolic Analysis of Relay and Switching Circuits." *Electrical Engineering* 57 (12): 713–723. doi:10.1109/EE.1938.6431064.

Shruthi, R. B. V., N. Kerle, V. Jetten, and A. Stein. 2014. "Object-Based Gully System Prediction from Medium Resolution Imagery Using Random Forests." *Geomorphology* 216: 283–294. doi:10.1016/j.geomorph.2014.04.006.

Smith, A. 2010. "Image Segmentation Scale Parameter Optimization and Land Cover Classification Using the Random Forest Algorithm." *Journal of Spatial Science* 55: 69–79. doi:10.1080/14498596.2010.487851.

Stumpf, A., and N. Kerle. 2011. "Object-Oriented Mapping of Landslides Using Random Forests." *Remote Sensing of Environment* 115 (10): 2564–2577. doi:10.1016/j.rse.2011.05.013.

Tiede, D., S. Lang, F. Albrecht, and D. Hölbling. 2010. "Object-Based Class Modeling for Cadastre-Constrained Delineation of Geo-Objects. Photogramm." *Photogrammetric Engineering & Remote Sensing* 76 (2): 193–202. doi:10.14358/PERS.76.2.193.

Tsai, Y. H., D. Stow, and J. Weeks. 2011. "Comparison of Object-Based Image Analysis Approaches to Mapping New Buildings in Accra, Ghana Using Multi-Temporal QuickBird Satellite Imagery." *Remote Sensing* 3 (12): 2707–2726. doi:10.3390/rs3122707.

Tuia, D., F. Ratle, F. Pacifici, M. F. Kanevski, and W. J. Emery. 2009. "Active Learning Methods for Remote Sensing Image Classification." *IEEE Transactions on Geoscience and Remote Sensing* 47 (7): 2218–2232. doi:10.1109/TGRS.2008.2010404.

Tuia, D., M. Volpi, L. Copa, M. Kanevski, and J. Munoz-Mari. 2011. "A Survey of Active Learning Algorithms for Supervised Remote Sensing Image Classification." *IEEE Journal of Selected Topics in Signal Processing* 5 (3): 606–617. doi:10.1109/JSTSP.2011.2139193.

Verbeeck, K., M. Hermy, and J. V. Orshoven. 2012. "External Geo-Information in the Segmentation of VHR Imagery Improves the Detection of Imperviousness in Urban Neighbourhoods." *International Journal of Applied Earth Observation & Geoinformation* 18 (18): 428–435. doi:10.1016/j.jag.2012.03.015.

Verikas, A., A. Gelzinis, and M. Bacauskiene. 2011. "Mining Data with Random Forests: A Survey and Results of New Tests." *Pattern Recognition* 44 (2): 330–349. doi:10.1016/j.patcog.2010.08.011.

Welch, B. L. 1947. "The Generalisation of Student's Problems When Several Different Population Variances are Involved." *Biometrika* 34 (1–2): 28.

Weszka, J. S., C. R. Dyer, and A. Rosenfeld. 1976. "A Comparative Study of Texture Measures for Terrain Classification." *IEEE Transactions on Systems Man & Cybernetics* 6 (4): 269–285. doi:10.1109/TSMC.1976.5408777.

Whiteside, T. G., S. W. Maier, and G. S. Boggs. 2014. "Area-Based and Location-Based Validation of Classified Image Objects." *International Journal of Applied Earth Observation and Geoinformation* 28 (1): 117–130. doi:10.1016/j.jag.2013.11.009.

Witharana, C., and D. L. Civco. 2014. "Optimizing Multi-Resolution Segmentation Scale Using Empirical Methods: Exploring the Sensitivity of the Supervised Discrepancy Measure Euclidean Distance 2 (ED2)." *ISPRS Journal of Photogrammetry & Remote Sensing* 87 (1): 108–121. doi:10.1016/j.isprsjprs.2013.11.006.

Witharana, C., D. L. Civco, and T. H. Meyer. 2014. "Evaluation of Data Fusion and Image Segmentation in Earth Observation-Based Rapid Mapping Workflows." *ISPRS Journal of Photogrammetry & Remote Sensing* 87 (2014): 1–18. doi:10.1016/j.isprsjprs.2013.10.005.

Wu, Y., I. Kozintsev, J. Bouguet, and C. Dulong. 2006. "Sampling Strategies for Active Learning in Personal Photo Retrieval." In 2006 IEEE International Conference on Multimedia and Expo, 529–532. Penang, Malaysia.

Yang, Q., and W. Kang. 2009. "General Research on Image Segmentation Algorithms." *International Journal of Image Graphics & Signal Processing* 1 (1): 1–8. doi:10.5815/ijigsp.

Zhang, L., L. Zhang, D. Tao, and X. Huang. 2012. "On Combining Multiple Features for Hyperspectral Remote Sensing Image Classification." *IEEE Transactions on Geoscience and Remote Sensing* 50 (3): 879–893. doi:10.1109/TGRS.2011.2162339.

Zhang, X. L., P. F. Xiao, X. Q. Song, and J. F. She. 2013. "Boundary-Sonstrained Multi-Scale Segmentation Method for Remote Sensing Images." *ISPRS Journal of Photogrammetry and Remote Sensing* 78 (4): 15–25. doi:10.1016/j.isprsjprs.2013.01.002.

Zhang, X. L., X. Z. Feng, P. F. Xiao, G. J. He, and L. J. Zhu. 2015. "Segmentation Quality Evaluation Using Region-Based Precision and Recall Measures for Remote Sensing Images." *ISPRS Journal of Photogrammetry and Remote Sensing* 102: 73–84. doi:10.1016/j.isprsjprs.2015.01.009.